View metadata, citation and similar papers at core.ac.uk

brought to you by CORE

provided by Archivio della ricerca - Università degli studi di Napoli Federico II

Cholesteatoma vs granulation tissue: a differential diagnosis by DWI-MRI apparent diffusion coefficient

M. Cavaliere, Antonella Miriam Di Lullo, E. Cantone, G. Scala, A. Elefante, C. Russo, L. Brunetti, G. Motta & M. Iengo

European Archives of Oto-Rhino-Laryngology
and Head & Neck

ISSN 0937-4477
Volume 275
Number 9

Eur Arch Otorhinolaryngol (2018)
275:2237-2243
DOI 10.1007/s00405-018-5082-5

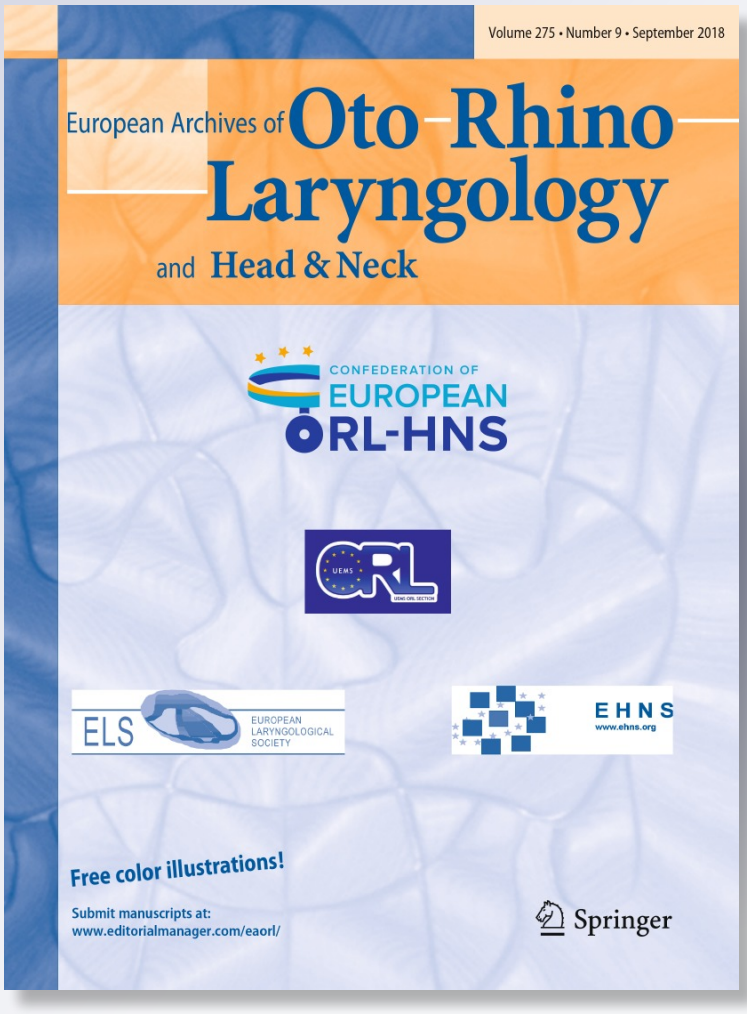

Springer

Your article is protected by copyright and all rights are held exclusively by Springer-Verlag GmbH Germany, part of Springer Nature. This e-offprint is for personal use only and shall not be self-archived in electronic repositories. If you wish to self-archive your article, please use the accepted manuscript version for posting on your own website. You may further deposit the accepted manuscript version in any repository, provided it is only made publicly available 12 months after official publication or later and provided acknowledgement is given to the original source of publication and a link is inserted to the published article on Springer's website. The link must be accompanied by the following text: "The final publication is available at link.springer.com".

Author's personal copy

European Archives of Oto-Rhino-Laryngology (2018) 275:2237–2243
https://doi.org/10.1007/s00405-018-5082-5

OTOLOGY

Cholesteatoma vs granulation tissue: a differential diagnosis by DWI-MRI apparent diffusion coefficient

M. Cavaliere[1] · Antonella Miriam Di Lullo[1] · E. Cantone[1] · G. Scala[2] · A. Elefante[3] · C. Russo[3] · L. Brunetti[3] · G. Motta[1] · M. Iengo[1]

Received: 10 April 2018 / Accepted: 31 July 2018 / Published online: 7 August 2018
© Springer-Verlag GmbH Germany, part of Springer Nature 2018

Abstract

Purpose To diagnose cholesteatoma when it is not visible through tympanic perforation, imaging techniques are necessary. Recently, the combination of computed tomography and magnetic resonance imaging has proven effective to diagnose middle ear cholesteatoma. In particular, diffusion weighted images have integrated the conventional imaging for the qualitative assessment of cholesteatoma. Accordingly, the aim of this study was to obtain a quantitative analysis of cholesteatoma calculating the apparent diffusion coefficient value. So, we investigated whether it could differentiate cholesteatoma from other inflammatory tissues both in a preoperative and in a postoperative study.

Methods This study included 109 patients with clinical suspicion of primary or residual/recurrent cholesteatoma. All patients underwent preoperative computed tomography and magnetic resonance imaging with diffusion sequences before primary or second-look surgery to calculate the apparent diffusion coefficient value.

Results We found that the apparent diffusion coefficient values of cholesteatoma were significantly lower than those of non cholesteatoma. In particular, the apparent diffusion coefficient median value of the cholesteatoma group (0.84×10^{-3} mm^2/s) differed from the inflammatory granulation tissue (2.21×10^{-3} mm^2/s) group ($p<2.2\times10^{-16}$). Furthermore, we modeled the probability of cholesteatoma by means of a logistic regression and we determined an optimal cut-off probability value of ~0.86 (specificity = 1.0, sensitivity = 0.97), corresponding to an apparent diffusion coefficient cut-off value of 1.37×10^{-3} mm^2/s.

Conclusions Our study has demonstrated that apparent diffusion coefficient values constitute a valuable quantitative parameter for preoperative differentiation of cholesteatomas from other middle ear inflammatory diseases and for postoperative diagnosis of recurrent/residual cholesteatomas.

Keywords Cholesteatoma · Granulation tissue · Middle ear · Magnetic resonance imaging · Apparent diffusion coefficient (ADC).

Introduction

Cholesteatoma is a middle ear lesion consisting of squamous cells debris. It is locally aggressive and requires surgical treatment. Imaging techniques are needed when cholesteatoma is not visible through a tympanic perforation.

Computed tomography (CT) has proven to be very useful for evaluating the extent of the disease and visualizing ear landmarks. However, it can only provide indirect signs of cholesteatoma like bone erosion of crucial anatomical areas (e.g., tegmen tympani, scutum, and ossicular chain), showing low values of sensitivity (43%) and specificity (48%) for recurrent or residual cholesteatoma [1].

✉ Antonella Miriam Di Lullo
antonella.dilullo@libero.it

[1] Department of Neuroscience, Reproductive and Odontostomatologic Sciences, ENT Unit, University of Naples "Federico II", Pansini Street no. 5, 80131 Naples, Italy

[2] Institute of Biotechnology, University of Helsinki, Helsinki, Finland

[3] Department of Advanced Biomedical Sciences, University of Naples "Federico II", Pansini Street no. 5, 80131 Naples, Italy

Author's personal copy

Recently, the combination of CT and Magnetic Resonance Imaging (MRI) has remarkably improved the diagnostic accuracy of cholesteatoma. Conventional cholesteatoma MRI images per se only display non-specific intermediate signal intensities on T1-weighted imaging and hyperintense signal intensities on T2-weighted imaging without significant enhancement [2, 3]. More recently, the Diffusion Weighted Intensity (DWI)-MRI has thus integrated the conventional MRI to assess the nature of middle ear lesions [3–6]. However, the DWI-MRI technique represents only a qualitative evaluation tool, depending on the subjective evaluation of experienced radiologists [7]. Prior studies on qualitative DWI has showed high values of sensitivity, specificity, positive predictive values (PPV) and negative predictive values (NPV) for echo-planar (EPI) and non echo-planar (non-EPI) sequences as reported in systematic reviews written by Jindal et al. [8] and Muzaffar et al. [9]. Recently, reported ranges for EPI sequences are: sensitivity of 12.5–100%, specificity of 60–100%, PPV of 80–100%, NPV of 50–92%. Instead, reported ranges for non-EPI sequences are: sensitivity of 62–100%, specificity of 85.7–100%, PPV of 89–100%, NPV of 50–100% [9].

The purpose of this study was to perform a quantitative analysis of middle ear cholesteatoma. For this purpose, we applied the apparent coefficient diffusion (ADC) protocol to DWI-MRI to identify a numeric cut-off value that could differentiate cholesteatoma from other inflammatory tissue both in a preoperative and in a postoperative study, in a large sample size.

Materials and methods

Participants

This prospective study—carried out at the University of Naples "Federico II" (Naples, Italy) from April 2011 to March 2016—included 109 consecutive patients (62 females; 47 males; age range 10–70 years, mean age 35.6 years) with clinical suspicion of primary or residual/recurrent cholesteatoma.

Exclusion criteria were formal contraindications in performing MRI or patients' refusal to undergo MRI.

In our study, all patients underwent preoperative CT examination and MRI imaging of the petrous temporal bone within 1–2 weeks after CT examination, before primary or second-look surgery. Intraoperative observations, which established the presence of cholesteatoma and/or granulation tissue, were subsequently confirmed histologically. Cholesteatoma was confirmed in 77 (70.64%) cases, whereas granulation tissue was found in 32 (29.36%) cases. Fifty-eight subjects (53.21%), i.e., 38 (65.52%) with cholesteatoma and 20 (34.48%) with granulation tissue, underwent primary tympanoplasty; whereas 51 (46.79%) subjects, 39 (76.47%) with cholesteatoma and 12 (23.53%) with granulation tissue underwent second-look surgery. The mean ADC value, measured on the ADC map, was calculated on the basis of the DWI sequences obtained before surgery.

All participants gave their written informed consent to participate in the study, which was fully approved by the local Board of Medical Ethics.

Imaging

The CT examination, required routinely for all patients undergoing surgery, has been performed by the Toshiba Aquilion 64-slice equipment.

MRI examination was performed on a 1.5T MR unit (Philips Intera, Philips Medical Systems, ++Netherlands) with an 8-channel head coil. Conventional sequences and Multi–Shot Non-Echo Planar Diffusion Weighted Imaging (MSh non-EPI DWI − 20 slides; TR 3000 ms; TE 82.44 ms; matrix 160 × 160; voxel size 2338 × 1210; $b = 0$ and $b = 1000$ s/mm^2; 5 averages) were obtained on the coronal plane. In particular, DWI acquisition was performed with cardiac gating to limit patient-related artifacts. ADC maps were then obtained with the Osirix plugin "ADC Map Calculation"; the ADC value was calculated by placing a small region of interest (ROI) of 1 mm^2 in the part of the lesion with more evident water diffusion restriction. Our choice to use an ROI with a small diameter was dictated by the small size of the lesions considered and by the need to obtain numerical ADC values that could actually reflect cholesteatomas, thus minimizing the interference of surrounding tissues.

Whether ADC could differentiate cholesteatoma from other inflammatory tissue was established by the arithmetic mean of ADC values measured by three different neuroradiologists, respectively, 30 years-long (E.A.), 15 years-long (R.C.) and 5 years-long experience (B.L.) in head and neck imaging. Our radiologists were blinded in terms of surgical findings.

Statistical analysis

The distribution of ADC mean values of patients with histologically confirmed cholesteatoma was compared with that of patients with non-cholesteatomatous inflammatory lesions by means of Wilcoxon rank-sum test. A binomial logistic regression model was used to predict the probability of cholesteatoma and inflammation on the basis of the ADC values. In particular, a 10-fold cross-validation approach was used to assess the mean accuracy of the model and a final logistic model was trained on the whole dataset (average accuracy: 0.96, SD = 0.07).

Author's personal copy

To determine an optimal cut-off on the probability value, Youden's J statistic was applied to the ROC curve of the estimated probabilities—which were obtained by applying the computed logistic function to the 109 starting values. In general, the optimal cut-off is determined as the threshold that maximizes the distance to the identity (diagonal) line. A p value of 0.01 was considered statistically significant.

All statistical analyses were performed with R version 3.2.5 software (cit. R Core Team: R: A Language and Environment for Statistical Computing, R Foundation for Statistical Computing, Vienna, Austria: ISBN 3-900051-07-0, URL http://www.R-project.org/).

Results

We analyzed the distribution pattern of ADC values of a cholesteatoma and a granulation tissue group. The two groups were characterized by different ADC values (Fig. 1). Statistically strong differences in ADC values were found between cholesteatoma (median 0.84×10^{-3} mm^2/s) and granulation tissue (median 2.21×10^{-3} mm^2/s) (Wilcoxon rank-sum test, $p=4.88\times10^{-16}$) (Fig. 2).

Binomial logistic regression (intercept = 12.352, beta = −7.647) estimated the probability of cholesteatoma vs granulation tissue on the basis of the ADC values. An ROC

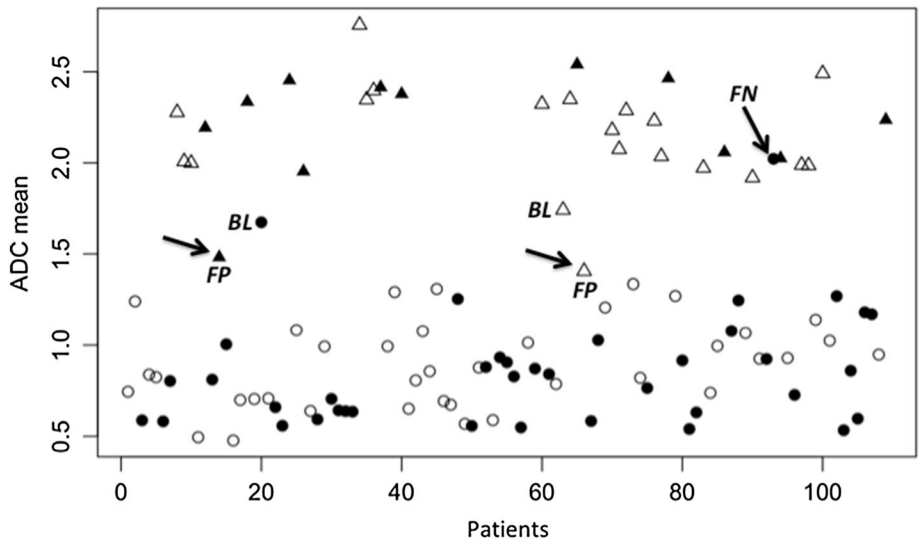

Fig. 1 The scatter plot represents the distribution of the ADC values between cholesteatoma and granulation tissue samples. There are three outliers: two false positive cases (FP) (number 14 and 66) and a false negative patient (FN) (number 93) (black arrows). Moreover two other patients resulted borderline (BL) (number 20 and 63). (unfilled circle: patient with cholesteatoma underwent tympanoplasty, filled circle: patient with cholesteatoma that underwent second-look surgery, unfilled triangle: patient with granulation tissue that underwent tympanoplasty, filled triangle: patient with granulation tissue that underwent second-look surgery)

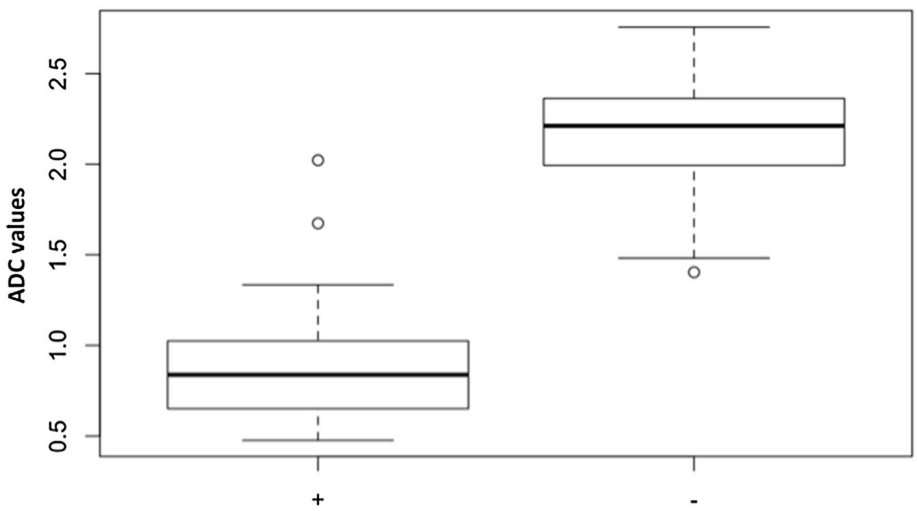

Fig. 2 The box plot represents the distribution pattern of ADC values of a cholesteatoma and a granulation tissue group. The two groups were characterized by different ADC values: cholesteatoma (median 0.84×10^{-3} mm^2/s) and granulation tissue (median 2.21×10^{-3} mm^2/s) (Wilcoxon rank-sum test, $p=4.88\times10^{-16}$). + (positive for cholesteatoma); − (negative for cholesteatoma)

Author's personal copy

curve evaluated the estimated probabilities, yielding an optimal cut-off value for the probability value of ~0.86 (specificity = 1.0 sensitivity = 0.97). This value corresponded to a cut-off ADC value of 1.37×10^{-3} mm^2/s (Fig. 3). This value corresponds the best threshold value that can be used to classify patients with cholesteatoma based on the trained regression model.

Moreover, according to the class-probability values provided by our model we could identify three outliers in our original dataset: two false positive cases (number 14 and 66) and a false negative patient (number 93). Moreover, two other patients resulted borderline (number 20 and 63) (Figs. 1, 2, 3).

Discussion

According to many authors [3–5, 10], DWI-MRI provides greater accuracy in differentiating cholesteatoma from other types of middle ear inflammation than standard CT, especially in second-look surgery. In fact, although CT scans are indeed valuable tools, they do show low diagnostic accuracy. For instance, Ganaha et al. [11], who evaluated the sensitivity and reliability of CT scans in detecting cholesteatomas, found that CT scans can provide accurate sensitivity, specificity, positive predictive values and negative predictive values only up to 71.1%, 78.5%, 93.3%, 39.2%, respectively.

Similarly, the sensitivity of echo planar DWI is highly variable, ranging from 12.5 to 86% [12, 13]. For instance, a study comprising 100 patients (55 primary cases with acquired cholesteatoma and 45 with residual cholesteatoma) reports a sensitivity rate of 81% for primary acquired cholesteatomas and 12.5% for residual cholesteatomas [12]. Very recent research further suggests the rather low and variable reliability of these sequences, reporting sensitivity, specificity, positive and negative predictive values of 86%, 87%, 92%, 77%, respectively [14]. The main limitation of echo-planar DWI sequences seems to be attributable to their inability to detect small cholesteatomas (< 5 mm) [15].

Contrary to echo-planar DWI, non-echo planar DWI appears more efficient in detecting cholesteatomas owing to its ability to detect cholesteatomas as small as 3 mm [13]. A recent systematic review of 8 studies with 207 subjects corroborates the higher reliability of non-planar DWI sequences by reporting a 91% sensitivity and 96% specificity for recurrent and residual cholesteatomas [8].

Overall, although these radiological images provide meaningful clinical information, their interpretation still remains rather subjective (Figs. 4, 5). Accordingly, the experience of neuroradiologists are paramount to interpret MRI imaging and to achieve accurate diagnosis of cholesteatomas.

To overcome these limitations and obtain a more complete, quantitative analysis of middle ear lesions, we applied the apparent coefficient diffusion (ADC) protocol to identify a numeric cut-off value that could differentiate cholesteatoma from inflammatory tissue especially after second-look surgeries. Indeed, after these types of surgical procedures a suspect lesion is more difficult to investigate both microscopically and otoendoscopically because of the reconstructed eardrum integrity.

So far, only few studies have underscored the importance of combining ADC values with DWI-MRI to differentiate with greater specificity cholesteatoma from other inflammatory diseases of the middle ear [16]. However, the small sample of these studies has been a major limitation [2].

To the best of our knowledge, this study embraces the largest sample size ever reported in the literature on the combination of DWI and estimated ADC values to differentiate cholesteatoma from other middle ear inflammatory diseases.

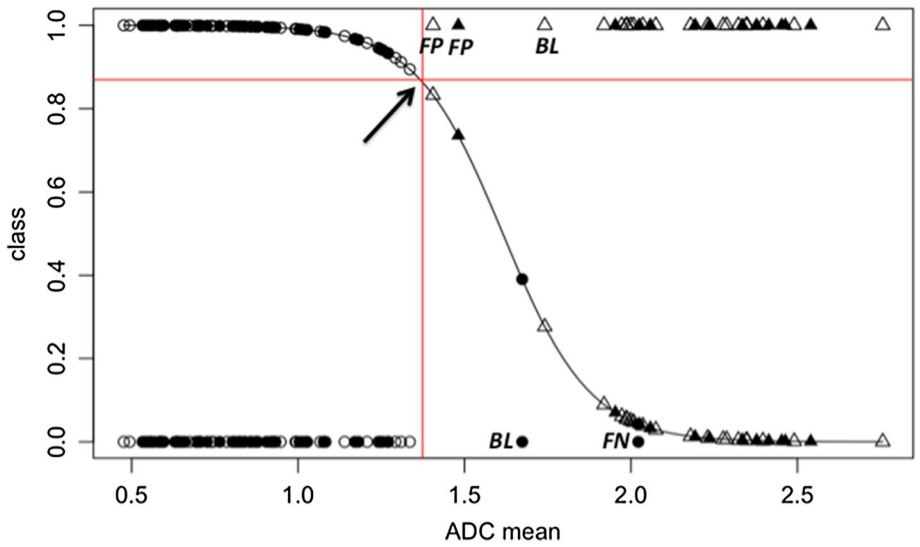

Fig. 3 Logistic model to predict the probability of pathological state (cholesteatoma or granulation tissue) given the ADC value. Optimal cut-off ADC value corresponded to 1.37×10^{-3} mm^2/s (black arrow). (unfilled circle: patient with cholesteatoma underwent tympanoplasty, filled circle: patient with cholesteatoma that underwent second-look surgery, unfilled triangle: patient with granulation tissue that underwent tympanoplasty, filled triangle: patient with granulation tissue that underwent second-look surgery, *FP* false positive cases, *FN* false negative cases, *BL* borderline cases)

Author's personal copy

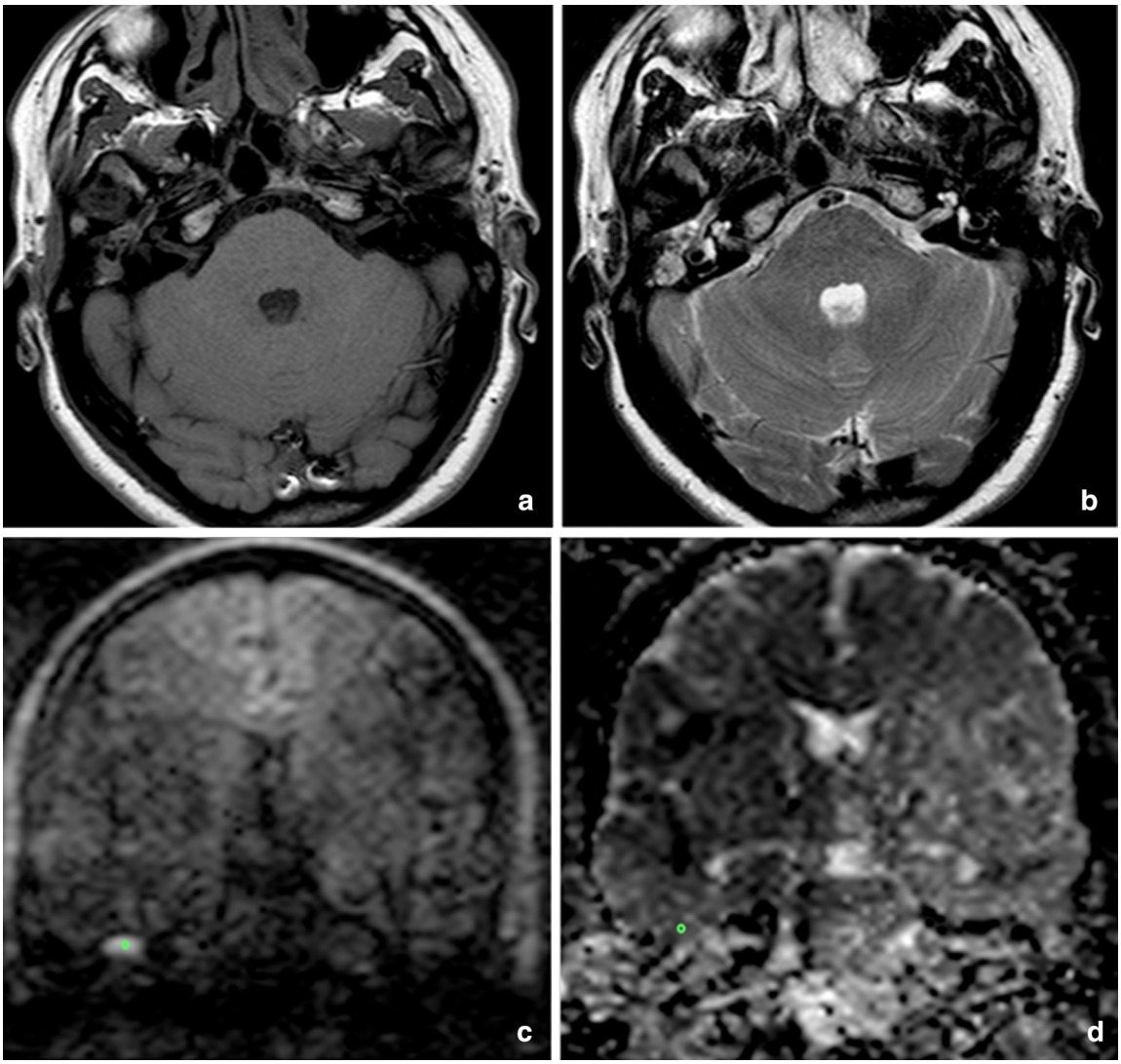

Fig. 4 Axial SE-T1w (**a**), axial TSE-T2w (**b**), coronal MSH-TSE DWI (**c**) with the calculated ADC value on ADC cartography (area: 1.000 mm^2; *W*: 1.000 mm × *H*: 1.000 mm; mean: 639×10^{-6} mm^2/s; min: 339×10^{-6} mm^2/s; max: 791×10^{-6} mm^2/s) (**d**) of a 40 year-old male patient with final diagnosis of right middle ear primary cholesteatoma

We found significant differences in ADC values between cholesteatoma and granulation tissue. This finding is supported by previous literature reporting that ADC values in cholesteatoma are significantly lower than those in other middle ear inflammatory diseases [7, 16].

In addition, using the logistic regression model, we were able to calculate an optimal ADC cut-off value (1.37×10^{-3} mm^2/s) to identify patients with cholesteatoma. This allowed us to identify cholesteatomas from the ADC values below our cut-off value with a high diagnostic accuracy (specificity = 1.0 sensitivity = 0.97). Remarkably, we misdiagnosed only three patients. In particular, we found one false negative and two false positive cases. The false negative was due to the small size of the cholesteatoma (< 3 mm)—as it was too small to be detected by DWI, even using non-EPI Multi-Shot (MSh) sequences [3, 17, 18]. Instead, the false positive patients were due to the presence of a superinfection, which generally decreases ADC values, as evidenced in a previous study reporting low ADC values in cases of middle ear abscess [2].

Conclusion

Despite the imbalanced nature of our sample—as it included more cholesteatomatous cases than non-cholesteatomatous ones—we have demonstrated that ADC values can provide a quantitative analysis of cholesteatoma even if it is not visible through tympanic perforation. DWI displayed significantly lower ADC values for cholesteatoma

Author's personal copy

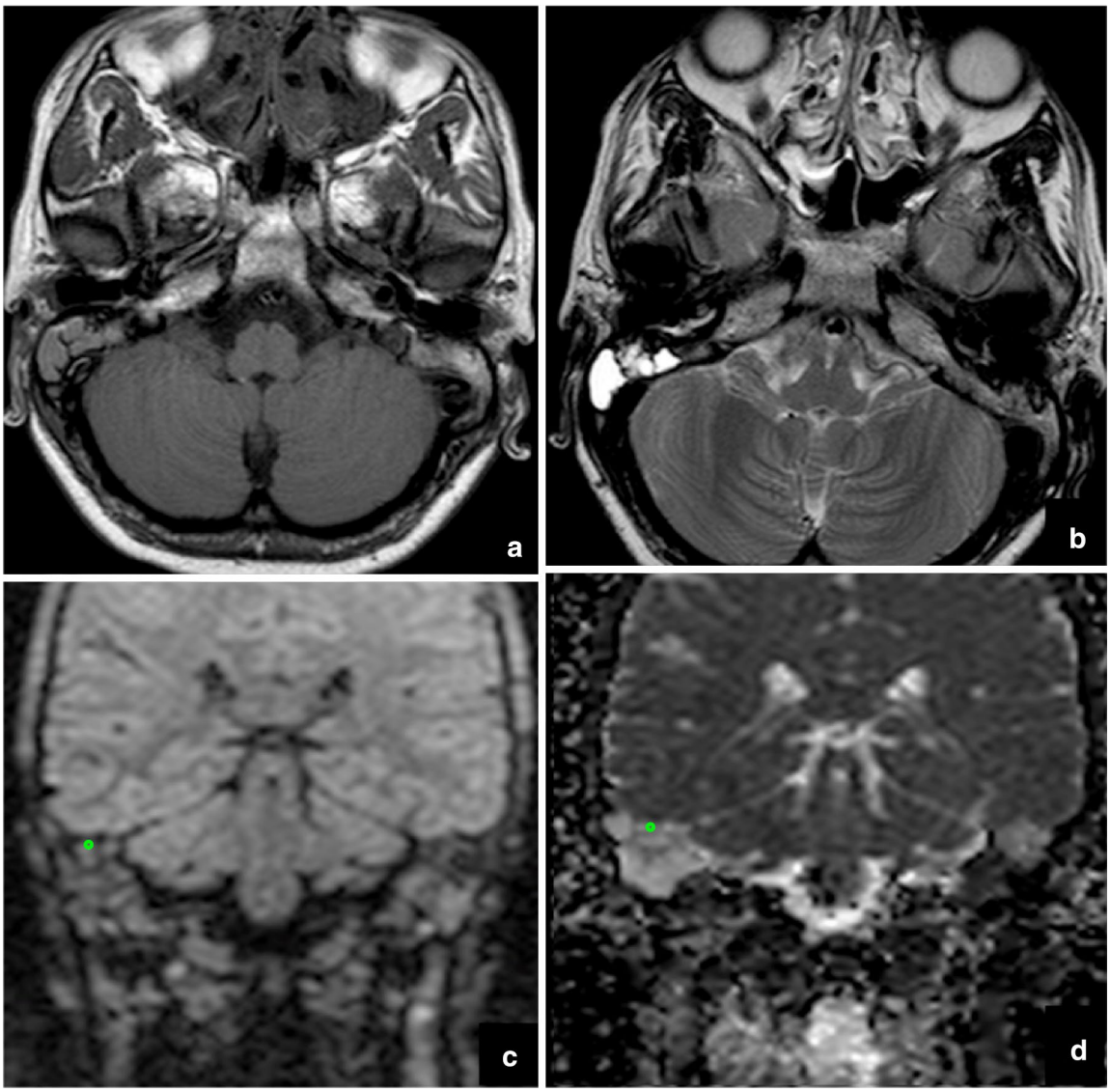

Fig. 5 Axial SE-T1w (**a**), axial TSE-T2w (**b**), coronal MSH-TSE DWI (**c**) with the calculated ADC value on ADC cartography (area: 1.000 mm^2; *W*: 1.000 mm × *H*: 1.000 mm; mean: 2277 × 10 − 6 mm^2/s; min: 2203 × 10 − 6 mm^2/s; max: 2341 × 10 − 6mm2/s) (**d**) of a 53 year-old female patient with final diagnosis of right middle ear non-cholesteatomatous granulation tissue

(median 0.84×10^{-3} mm^2/s) than for noncholesteatomatous tissue (median 2.21×10^{-3} mm^2/s). This finding suggests that the combination of a qualitative evaluation of DWI sequences andADC values can increase the diagnostic accuracy even of small-sized cholesteatomas, especially in post-operative follow-up cholesteatomas. In particular, our estimated ADC cut-off value of 1.37×10^{-3} mm^2/s allowed us to identify cholesteatoma from ADC values lower than our cut-off value with a high diagnostic accuracy (specificity = 1.0 sensitivity = 0.97).

Technological advances are nonetheless warranted to overcome one major shortcoming in this field of research: the limited sensitivity of current imaging techniques in detecting cholesteatomas less than 3 mm.

Compliance with ethical standards

Conflict of interest The authors have no funding, financial relationships, or conflicts of interest to disclose.

Author's personal copy

References

1. Tierney PA, Pracy P, Blaney SP et al (1999) An assessment of the value of the preoperative computed tomography scans prior to otoendoscopic 'second look' in intact canal wall mastoid surgery. Clin Otolaryngol Allied Sci 24:274–276
2. Thiriat S, Riehm S, Kremer S, Martin E, Veillon F (2009) Apparent diffusion coefficient values of middle ear cholesteatoma differ from abscess and cholesteatoma admixed infection. AJNR Am J Neuroradiol 30:1123–1126
3. Cavaliere M, Di Lullo AM, Caruso A et al (2014) Diffusion-weighted intensity magnetic resonance in the preoperative diagnosis of cholesteatoma. J Otorhinolaryngol Relat Spec 76:212–221
4. Maheshwari S, Mukherji SK (2002) Diffusion-weighted Imaging for differentiating recurrent cholesteatoma from granulation tissue after mastoidectomy: case report. AJNR Am J Neuroradiol 23:847–849
5. Li PM, Linos E, Gurgel RK, Fischbein NJ, Blevins NH (2013) Evaluating the utility of non-echo-planar diffusion-weighted imaging in the preoperative evaluation of cholesteatoma: a meta-analysis. Laryngoscope 123:1247–1250
6. Elefante A, Cavaliere M, Russo C et al (2015) Diffusion weighted MR imaging of primary and recurrent middle ear cholesteatoma: an assessment by readers with different expertise. BioMed Res Int 2015:597896
7. Lingam RK, Khatri P, Hughes J, Singh A (2013) Apparent diffusion coefficients for detecting of postoperative middle ear cholesteatoma on non-echo-planar diffusion-weighted images. Radiology 269:504–510
8. Jindal M, Riskalla A, Jiang D, Connor S, O' Connor AF (2011) A systematic review of diffusion-weighted magnetic resonance imaging in the assessment of postoperative cholesteatoma. Otol Neurotol 32:1243–1249
9. Muzaffar J, Metcalfe C, Colley S, Coulson C (2017) Diffusion-weighted magnetic resonance imaging for residual and recurrent cholesteatoma: a systematic review and meta-analysis. Clin Otolaryngol 42:536–543
10. Yigiter AC, Pinar E, Imre A, Erdoga N (2015) Value of echo-planar diffusion-weighted magnetic resonance imaging for detecting tympanomastoid cholesteatoma. J Int Adv Otol 11:53–57
11. Ganaha A, Outa S, Kyuuna A et al (2011) Efficacy of diffusion-weighted magnetic resonance imaging in the diagnosis of middle ear cholesteatoma. Auris Nasus Larynx 38:329–334
12. Vercruysse JP, De Foer B, Pouillon M, Somers T, Casselman J, Officiers E (2006) The value of diffusion-weighted MR imaging in the diagnosis of primary acquired and residual cholesteatoma: a surgical verified study of 100 patients. Eur Radiol 16:1461–1467
13. Jeunen G, Desloovere C, Hermans R, Vandecaveye V (2008) The value of magnetic resonance imaging in the diagnosis of residual or recurrent acquired cholesteatoma after canal wall-up tympanoplasty. Otol Neurotol 29:16–18
14. Dundar Y, Akcan FA, Dilli A, Tatar E, Korkmaz H, Ozdek A (2015) Does diffusion-weighted MR imaging change the follow-up strategy in cases with residual cholesteatoma? J Int Adv Otol 11:58–62
15. De Foer B, Vercruysse JP, Bernaerts A et al (2007) The value of single-shot turbo spin-echo diffusion-weighted MR imaging in the detection of middle ear cholesteatoma. Neuroradiology 49:841–848
16. Russo C, Elefante A, Di Lullo AM et al (2018) ADC benchmark range for correct diagnosis of primary and recurrent middle ear cholesteatoma. BioMed Res Int 2018:7945482
17. Huins CT, Singh A, Lingam RK, Kalan A (2010) Detecting cholesteatoma with non-echo planar (HASTE) diffusion-weighted magnetic resonance imaging. Otolaryngol Head Neck Surg 143:141–146
18. De Foer B, Vercruysse JP, Bernaerts A et al (2010) Middle ear cholesteatoma: non-echo-planar diffusion-weighted MR imaging versus delayed gadolinium-enhanced T1-weighted MR imaging-value in detection. Radiology 255:866–872